Monthly Notices
of the
ROYAL ASTRONOMICAL SOCIETY
MNRAS **445,** 1449–1461 (2014) doi:10.1093/mnras/stu1806

High-velocity blueshifted Fe II absorption in the dwarf star-forming galaxy PHL 293B: evidence for a wind driven supershell?

Roberto Terlevich,[1,2]★ Elena Terlevich,[1] Guillermo Bosch,[3,4] Ángeles Díaz,[5] Guillermo Hägele,[3,4] Mónica Cardaci[3,4] and Verónica Firpo[3,6]

[1]*INAOE, Luis Enrique Erro 1, Tonantzintla, Puebla, C.P. 72840, México*
[2]*Institute of Astronomy, Madingley Rd, Cambridge, CB3 0HA, UK*
[3]*Instituto de Astrofísica de La Plata (CONICET-UNLP), B1900FWA, La Plata, Argentina*
[4]*Facultad de Cs. Astronómicas y Geofísicas, UNLP, B1900FWA, La Plata, Argentina*
[5]*Departamento de Física Teórica, Universidad Autónoma de Madrid, Cantoblanco, E-28049 Madrid, Spain*
[6]*Departamento de Física, Universidad de la Serena, Av. Juan Cisternas 1200 Norte, La Serena, Chile*

Accepted 2014 September 2. Received 2014 September 2; in original form 2014 May 14

ABSTRACT

X-shooter and WHT-ISIS spectra of the star-forming galaxy PHL 293B also known as A2228-00 and SDSS J223036.79-000636.9 are presented in this paper. We find broad (FWHM = 1000 km s^{-1}) and very broad (FWZI = 4000 km s^{-1}) components in the Balmer lines, narrow absorption components in the Balmer series blueshifted by 800 km s^{-1}, previously undetected Fe II multiplet (42) absorptions also blueshifted by 800 km s^{-1}, IR Ca II triplet stellar absorptions consistent with [Fe/H] < -2.0 and no broad components or blueshifted absorptions in the He I lines. Based on historical records, we found no optical variability at the 5σ level of 0.02 mag between 2005 and 2013 and no optical variability at the level of 0.1 mag for the past 24 yr. The lack of variability rules out transient phenomena like luminous blue variables or Type IIn supernovae as the origin of the blueshifted absorptions of H I and Fe II. The evidence points to either a young and dense expanding supershell or a stationary cooling wind, in both cases driven by the young cluster wind.

Key words: galaxies: abundances – galaxies: dwarf.

1 INTRODUCTION

Early studies of emission line galaxies have shown that objects that spectroscopically resembled H II regions both in line emission intensities and widths, constituted about 80 per cent of total samples, the rest being galaxies of Seyfert type (see e.g. French 1980, and references therein). Some of these objects are also characterized by their compacticity and blue excess as shown on photographic plates and represent the overlap between blue compact galaxies (BCG) and H II galaxies. PHL 293B is one of these objects. It was found by Haro & Luyten (1962) in the 'Palomar–Haro–Luyten' survey of faint blue objects. Kinman (1965) obtained its optical spectrum and described it as having a faint continuum with unresolved emission in the Balmer series and [O III] λλ5007, 4959 and 4363 Å that makes of it, to our knowledge, one of the first detections of the [O III] λ4363 Å auroral line in a star-forming galaxy. We nowadays recognize this fact as the one allowing a trustworthy derivation of the gas elemental abundances in regions of star formation showing an emission line spectrum. In the case of PHL 293B, these abundances are amongst the lowest known, less than one-tenth of the solar value (French 1980; Izotov, Thuan & Stasińska 2007; Asplund et al. 2009) and in the border line of what is considered to be an extremely metal deficient galaxy (e.g. Kunth & Östlin 2000). The galaxy was included in the sample studied by French (1980) who lists its absolute magnitude and size as −13.6 and 0.2 kpc, respectively. PHL 293B also looks compact in the images obtained by Cairós et al. (2001), and Geha et al. (2006) give an effective radius for this galaxy of only 0.4 kpc. Its absolute magnitude according to the Sloan Digital Sky Survey (SDSS) is, $M_g = -14.77$. These facts make of it a very low luminosity and compact H II galaxy.

One of the characteristics of H II galaxies is their high star formation rate that takes place in a very small volume and probably in short duration episodes, thus making these galaxies easily observable. Given the large value of the equivalent width (EW) of their emission lines, it is the current burst of star formation that dominates their luminosity at blue and visible wavelengths. The low metallicity of these objects guarantees that they are in a chemically unevolved stage probably similar to what is expected in galaxies

★ E-mail: rjt@ast.cam.ac.uk

at early cosmological times. The evolution of their massive young stars, responsible for the gas ionization, is conditioned by their low metallicity as is probably the case for Pop III stars. The evolution of high-mass stars is short and encompasses phases with intense episodes of mass-loss; therefore, the presence of low-intensity broad components or wings in the otherwise narrow emission lines typical of star-forming regions (SFRs) are relatively common in high-S/N medium resolution spectra. Well-known examples are: NGC 604, a giant H II region in the spiral galaxy M 33 (Díaz et al. 1987; Terlevich et al. 1996); NGC 5471, a giant H II region in the spiral galaxy M 101 (Castañeda, Vilchez & Copetti 1990); NGC 2363, a giant H II region in the irregular galaxy NGC 2366 (Roy et al. 1992; González-Delgado et al. 1994); and 30 Dor in the Large Magellanic Cloud (LMC), one of the largest extragalactic H II regions in the local universe (Melnick, Tenorio-Tagle & Terlevich 1999). This is also the case, as expected, for H II galaxies and strong line BCG (see e.g. Izotov et al. 1996), since it is the dominant SFR that dominates their integrated spectra.

The most likely origin of the extended line wings observed in SFR is related to the evolution of very massive stars and the feedback processes between them and the surrounding interstellar medium (ISM). Given the large number of these stars present in a relatively small volume, it may be expected that the combination of their powerful winds gave rise to complex kinematical components in both permitted and forbidden lines. Also, multiple supernova events have been invoked as the possible cause (see Roy et al. 1992, for the case of NGC 2363). However, some of these massive stars like luminous blue variables (LBVs) can be so luminous as to be capable of producing visible effects by themselves particularly in nearby resolved system and some of them may even end their lives as supernovae, hence dominating for some time the galaxy luminosity output. This evolutionary path may be the one followed by the most massive stars of low metallicity for which the inefficiency of line-driven stellar winds would translate in a low mass-loss rate and failure in becoming a Wolf–Rayet (WR) star. Some of these stars might be the progenitors of Type IIn supernovae (SNe IIn) in which the narrow line spectrum arises from the interaction of the supernova blast wave with the circumstellar shell. These supernovae can be very luminous and also very long lived (Aretxaga et al. 1999; Smith, Fanelli & Marcum 2007).

Another mechanism accounting for the presence of low-intensity broad line components in H II galaxies or BCG spectra may be mass accretion on to an intermediate-mass black hole (10^3–10^5 $M_\odot$). Up to now there are no bona fide low-metallicity objects (about one-tenth of solar) harbouring massive black holes. In fact, it is intrinsically difficult to identify these objects in commonly used diagnostic diagrams (e.g. Stasińska et al. 2006). The overlapping of their broad component Hα luminosities and those of supernovae and even stellar winds, makes this identification even harder. Yet, from the point of view of galactic evolution to firmly establish the existence of these objects would be of the greatest importance. In this sense, the detection of X-rays emission would be a major discriminant.

In this work, we analyse recently obtained moderate- to high-resolution spectra of PHL 293B which is a low-luminosity, low-metallicity H II galaxy that shows low-intensity broad wings and blueshifted narrow absorptions in the hydrogen recombination lines, in order to try to shed some light on their origin. Section 2 gives a description of the data, Section 3 presents the results obtained from them and Section 4 is devoted to their analysis. A discussion is presented in Section 5 and the conclusions of our work are given in Section 6.

2 DESCRIPTION OF THE DATA

PHL 293B, also known as HL 293B, Kinman's dwarf, A2228-00 and SDSS J223036.79-000636.9, is a very low luminosity galaxy ($M_B = -14.37$; Cairós et al. 2001) at a distance of 23.1 Mpc obtained from the radial velocity (Mould et al. 2000) taken from NASA/IPAC Extragalactic Database (NED) corrected for Virgo Infall, Great Attractor and Shapley, with a Hubble constant of 73 km s^{-1} Mpc^{-1}. Its metallicity was first measured by French (1980) who gave a value of 12+log(O/H) = 7.78 and, more recently, by Izotov et al. (2007) who derive a value of 12+log(O/H) = 7.66 from SDSS data.

2.1 Spectroscopic data

We have compiled spectroscopic data of PHL 293B for four different epochs spanning more than 10 yr. Archival spectroscopic data have been extracted from DR7 of the SDSS (J223036.79-000636.9; Abazajian et al. 2009); European Southern Observatory (ESO) Very Large Telescope-UV Echelle Spectrograph (VLT-UVES) [Programme ID 70.B-0717(A)]; Science Verification (SV) VLT-X-shooter [ESO Programme ID 60.A-9442(A)]. To these data we have added new observations obtained with the ISIS spectrograph attached to the 4.2 m WHT at the Observatorio del Roque de los Muchachos in the island of La Palma (Spain).

The data from SDSS were taken on 2001 August 22 and cover the spectral range from 3800 to 9200 Å at a resolution $R = 1800$–2200. The UVES data were obtained on 2002 November 18 in both the blue and red arms covering a total wavelength range from 3100 to 6800 Å with 0.2 Å spectral resolution. X-shooter (Vernet et al. 2011) observations were performed during SV on the nights of 2009 August 16 and September 28. The data simultaneously cover the spectral range from UV(∼3000 Å) to K′ (∼2.5 μm) and were reduced using the ESO Recipe Execution Tool (ESOREX) following standard procedures with minor adaptations for these SV data.

ISIS data were obtained on 2011 November 30 using an EEV12 detector attached to the blue arm of the spectrograph. The R300B grating was used covering the unvignetted wavelength range 4800–7200 Å (centred at $\lambda_c = 6000$ Å), giving a spectral dispersion of 0.86 Å pixel^{-1} which combined with a slit width of 1 arcsec yields a resolution of about 3.4 Å. The observations were made at parallactic angle, at an airmass of 1.3 and with a seeing of 0.5 arcsec. Several bias and sky flat-field frames were taken at the beginning and at the end of the night. In addition, two lamp flat-fields, before and after the observation, and one calibration lamp exposure were performed. The calibration lamp used was CuNe+CuAr. The spectra were processed and analysed with IRAF routines[1] following standard procedures that include removal of cosmic rays, bias subtraction, division by a normalized flat-field and wavelength calibration. In the last step, the spectra were corrected for atmospheric extinction and flux calibrated. Four standard star observations were used: BD+17 4708, Wolf1346, G191B2B and Feige34 allowing a good spectrophotometric calibration with an estimated accuracy of about 5 per cent.

2.2 Photometric data

The photometric optical data were compiled from three different sources. The Catalina Sky Survey (CSS) second release (Drake

[1] IRAF: the Image Reduction and Analysis Facility is distributed by the National Optical Astronomy Observatories, which is operated by the Association of Universities for Research in Astronomy, Inc. (AURA) under cooperative agreement with the National Science Foundation (NSF).

et al. 2009) provides for PHL 293B, accurate magnitudes for 80 nights from 2005 April to 2012 October. Most nights have four different observations inside one hour total observing time. In addition, the SDSS provides photometric parameters for the night of 2001 August 22, and Cairós et al. (2001) published their photometry for PHL 293B obtained in 1988 October with the 3.5 m telescope of the Calar Alto Observatory (Spain). Kinman (1965) provides the earliest brightness estimates based on the Palomar Sky Survey (PSS) plates and photographic images taken with the Lick Observatory 20-inch Astrograph in 1949 and 1965 and at the prime focus of the Lick 120-inch telescope.

PHL 293B was observed also using the ACIS-S camera on board the *Chandra X-ray Observatory* on 2009 September 25. Data cover the energy range 0.4–10 keV and the exposure time was about 7.7 ks (ObsID 11294).

3 RESULTS

3.1 Spectroscopy

The blue to visual spectrum of PHL 293B shows the usual strong emission lines found in star-forming galaxies: recombination lines from hydrogen and helium and collisionally excited lines of different ions – [O II], [O III], [N II], [S II], [S III], etc. The most striking feature of the spectral lines is the presence of broad components in the hydrogen recombination lines, already reported by Izotov et al. (2007), which are undetected in the corresponding helium lines. These broad components that can be seen in Figs 1 through 5 for the Balmer lines, Hα, Hβ, Hγ and Hδ, have full width at half-maximum (FWHM) between 1000 and 400 km s^{-1} (Izotov & Thuan 2009; Izotov et al. 2011) and relatively low intensities. They are redshifted by about 50 km s^{-1} with respect to the narrow emission lines reference frame as determined by the centroid of the [O III] λ4959 Å line. Fig. 2 shows a detail of the multi-Gaussian fit performed on the X-shooter spectrum Hα profile. Details of measurements performed in SDSS and X-shooter spectra are listed in Tables 1 and 2, using the normal notation for EWs as positive for lines in absorption, negative for emission. In what follows, we will call the reference frame defined by the [O III] λ4959 Å line, the galaxy reference frame. The fluxes in the narrow component of Hα and Hβ (measured from the SDSS spectrum) are 4.86 and 1.54 $\times$ 10^{-14} erg s^{-1} cm^{-2}, respectively, and the ratio of broad to narrow components in both lines is about 0.25.

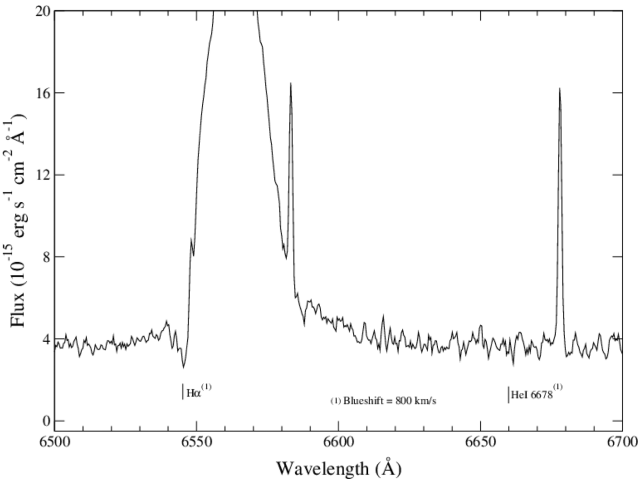

Figure 1. X-shooter spectrum showing the line profile around Hα. Here and in the following spectra, flux is measured in erg s^{-1} cm^{-2}.

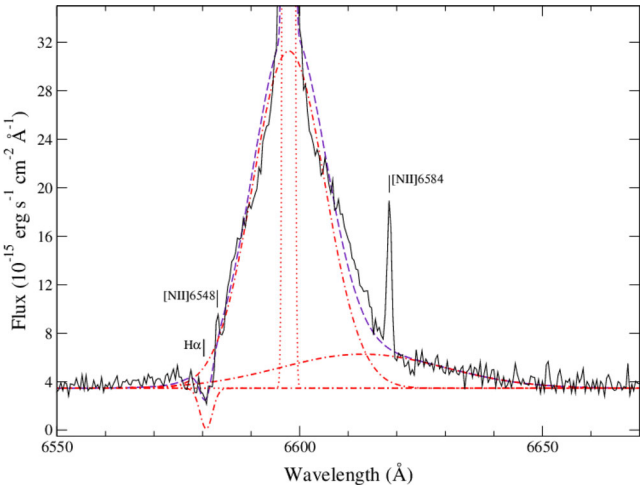

Figure 2. X-shooter spectrum showing the multi-Gaussian fit performed to the Hα line profile. Four components are clearly identified: a blue wing absorption blueshifted by 800 km s^{-1}, a strong narrow component, a strong broad component and a relatively fainter ultra-broad component, redshifted by 900 km s^{-1}. The narrow spike at λ6620 Å is an artefact from the reduction process and discarded during profile fitting.

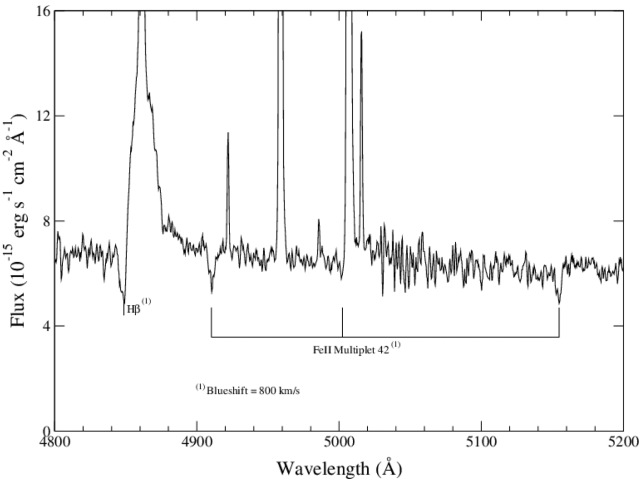

Figure 3. Same as Fig. 1, for the Hβ, [O III] λ5007 Å region. Note the possibly very broad blue wing in [O III]. The position of the Fe II multiplet 42 blueshifted by 800 km s^{-1} with respect to the galaxy rest frame is shown.

Errors in measurements depend strongly on flux uncertainties. Individual errors are determined from profile fitting routines. These errors rely on a good determination of errors present in the spectra, which is directly obtained for the SDSS spectra and had to be modelled for the X-shooter data. They are below 1 per cent for radial velocity and 10 per cent for dispersion determinations in strong narrow line profiles but can raise to tens of km s^{-1} for broader components. Uncertainties in flux range from 3 per cent in strong lines and/or components but can grow up to 20 per cent in weak absorption lines. EWs share a few per cent to 20 per cent uncertainty based on relatively low counts level for the continuum flux.

From the X-shooter data the measured narrow line Hα and Hβ fluxes are 2 and 0.66 $\times$ 10^{-14} erg s^{-1} cm^{-2}, respectively. The ratio Hα/Hβ between the narrow line components is the same in both spectra within the observational errors. The ratio between the narrow

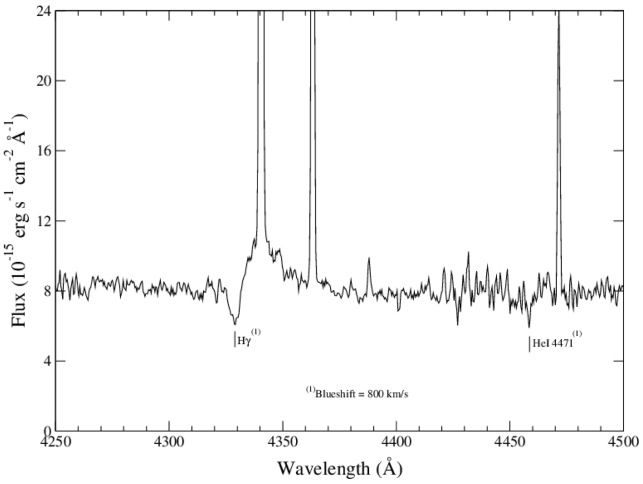

Figure 4. As Fig. 1, for Hγ. The positions of Hγ and He I λ4471 Å blueshifted by 800 km s^{-1} with respect to the galaxy rest frame are shown.

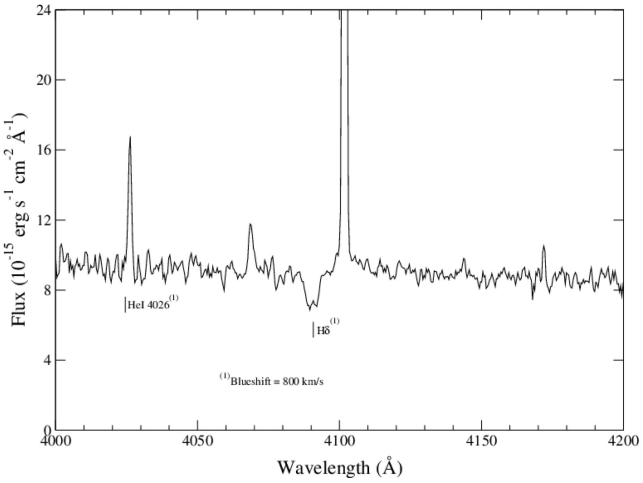

Figure 5. As Fig. 1, for Hδ. The positions of Hδ and He I λ4026 Å blueshifted by 800 km s^{-1} with respect to the galaxy rest frame are shown.

and broad components for these lines are also the same within the observational errors. Hence, the differences in the flux measurements between the SDSS and the X-shooter spectra can be attributed to aperture effects. Since the aperture used for the SDSS observations is larger than the one used for the X-shooter one, we hereafter use the SDSS measurements for the line fluxes and EWs. Additional features of the Balmer lines are an ultra-broad component with FWZI(full width at zero intensity) $\sim$4000 km s^{-1} redshifted by about 500 km s^{-1} and a P Cygni-like absorption blueshifted by 800 km s^{-1} with respect to the reference frame (see Table 2).

To summarize, the complex Hα line profile shows a narrow component at the galaxy reference frame, a broad component FWHM $\sim$ 1000 km s^{-1} redshifted by about 50 km s^{-1} with respect to the galaxy reference frame, an ultra-broad component with FWZI $\sim$ 4000 km s^{-1} redshifted by about 500 km s^{-1} and a P Cygni-like narrow absorption blueshifted by 800 km s^{-1}.

These features are also seen in the other Balmer lines, except for the ultra-broad component which is seen only as a red wing. A weak red wing is also visible in [O III] λ5007 Å corresponding possibly to the ultra-broad component. All these features are visible both in the X-shooter data analysed here and in the SDSS spectrum. The broad component represents about 20 per cent of the total Hα emission flux. The blueshifted absorption is weaker in Hα than in the other Balmer lines, although the continuum is difficult to fit in the blue wing of Hα.

The He I lines show only narrow components.

We have identified a conspicuous absorption feature at λ5183 Å. This absorption line has no emission counterpart and coincides with the wavelength of the Fe II multiplet 42 (laboratory wavelength 5169.03 Å) line blueshifted by the same 800 km s^{-1} displayed by the Balmer P Cygni-like components. Companion lines of the same multiplet blueshifted by the same velocity have also been found at $\lambda\lambda$5031, 4939 Å and they are indicated in Fig. 3. Further absorption lines are observed in the far red spectral region, corresponding to the Ca II triplet (CaT) lines at $\lambda\lambda$8498, 8542 and 8662 Å in the galaxy rest frame (see Fig. 6). Although these lines, being close to the left of the adjacent Paschen lines at $\lambda\lambda$8505, 8548 and 8667 Å, can mimic P Cygni profiles, the Ca II lines are clearly separated from the Paschen ones. Furthermore, there is no hint of a P Cygni-like component in the λ8601 Å Paschen line.

Although the X-shooter infrared spectrum is not a very good one, we can identify hydrogen recombination lines of the Paschen and Brackett series, He I lines and a hint of the H_2 line at 2.122 µm rest frame. There is no evidence for broad components or P Cygni-like profiles in any of these lines.

The WHT-ISIS spectrum covering from λ4300 Å to λ7500 Å (observations setup described in Section 2.1) is shown in Fig. 7. The strongest emission lines are labelled.

3.2 Photometry

We have extracted from the CSS data release 2 data base (Drake et al. 2009) 353 photometric points for PHL 293B corresponding to 91 observing nights over the 8.4 yr from 2005 May 16 to 2013 September 27. Most nights have four independent observations inside a 60 min total span. Nightly averages are shown (plus symbols) in Fig. 8 and have a typical rms scatter of 0.040 mag. The yearly averages are shown with filled rhomboids. The average brightness for the whole data set, indicated with a thin line, is $\langle V \rangle = 17.056 \pm 0.004$.

The SDSS published Petrosian r magnitude is $P_r = 17.04 \pm 0.01$ which combined with the colour $g - r = 0.03$ and the SDSS colour transformations yield a Petrosian v magnitude $P_v = 17.07 \pm 0.01$ observed on 2001 August 22. The SDSS value is indicated with an x in Fig. 8.

Cairós et al. (2001) provided an earlier photometric point for the object. Their 1988 October observation with the 3.5 m telescope of the Calar Alto Observatory gives $V = 17.02 \pm 0.01$.

Kinman (1965) published the earliest magnitude estimates for PHL 293B: $m_{pg} = 16.7$. We quote from his paper: 'a very rough estimate of the B magnitude is 17.7 on the Sky Survey plates and about a half magnitude fainter on the 120-inch plates'. Kinman attributes this difference to the scale difference between the PSS and the Lick 120-inch plates given that there is no variability between 1949 and 1965 in plates taken with the Lick 20-inch Astrograph. Bearing in mind that they are based on eye estimates of the PSS plates from 1949 and photographic images taken at the prime focus of the Lick Observatory 120-inch telescope in 1965, errors of about $\pm$0.5 mag are expected.

There is no detection of X-rays emission in the ACIS-*Chandra* image. The point source sensitivity of this camera in the 0.4–6 keV energy range is 4×10^{-15} erg cm^{-2} s^{-1} for an exposure time of 10 ks (table 6.1 of The *Chandra* Proposers' Observatory Guide

Table 1. SDSS spectroscopy: column 1 lists the line identification and its measured wavelength is included in column 2. Derived radial velocities are shown in column 3 and observed velocity dispersion, corrected by instrumental broadening, are listed in column 4. Errors in columns 2–4 are shown in parentheses, in km s^{-1}. Also, fluxes and equivalent widths (positive in absorption, negative in emission) of line profiles are shown in columns 5 and 6, respectively. Relative errors, in percentage, are shown in parentheses. Note that no errors are shown for the Fe II(42)5018 line because the close proximity of the strong He I line prevented the iterative fitting procedure (indicated by : symbol).

Id.	λ_{obs} (Å)	Radial vel. (km s^{-1})	σ_{obs} (km s^{-1})	Flux (10^{14} erg s^{-1} cm^{-2})	EW (Å)
Fe II(42) 1 λ4924	4939.6 (0.5)	955 (31)	133 (33)		1.0 (23 per cent)
Fe II(42) 2 λ5018	5030.3	710:	56:		0.5:
Fe II(42) 3 λ5169	5183.0 (0.4)	810 (20)	33 (20)		0.67 (23 per cent)
Hγ	4364.6 (0.02)	1665 (1)	59 (2)	0.7 (1.5 per cent)	−36 (1.5 per cent)
Hβ (narrow)	4888.4 (0.01)	1672 (1)	25 (1)	1.5 (1.2 per cent)	−82 (1.2 per cent)
Hβ (broad)	4890.4 (0.5)	1793 (30)	321 (34)	0.3 (8 per cent)	−21 (8 per cent)
Hβ (absorption)	4874.6 (0.3)	818 (17)	302 (19)		1.1 (16 per cent)
Hα (narrow)	6599.5 (0.01)	1678 (1)	36 (1)	4.7 (0.5 per cent)	−489 (0.5 per cent)
Hα (broad)	6601.2 (0.7)	1756 (30)	681 (33)	1.3 (5 per cent)	−138 (5 per cent)
[O III] λ5007	5034.8 (0.01)	1675 (0.2)	18.3 (0.1)	8.6 (1 per cent)	−594 (1 per cent)

Table 2. X-shooter spectroscopy: column descriptions are similar to those in Table 1. Column 5 lists individual component fluxes relative to the total flux measured for the overall emission profile. The red wing component in the Hα profile is fitted with a fix width, so the error determinations of all its components are not reliable, and therefore not included.

Id.	λ_{obs} (Å)	Radial vel. (km s^{-1})	σ_{obs} (km s^{-1})	Flux (relative to total line flux)	EW (Å)
Hβ (absorption)	4874.1 (0.1)	789 (6)	130 (11)	− 0.01	2 (10 per cent)
Hβ (narrow)	4887.0 (0.01)	1582 (1)	26 (01)	0.84	−96 (3 per cent)
Hβ (broad)	4887.8 (0.2)	1629 (12)	466 (13)	0.19	−21 (2 per cent)
Fe II(42) 1 λ4924	4936.7 (0.2)	777 (12)	115 (15)		1 (12 per cent)
Fe II(42) 3 λ5169	5181.6 (0.2)	733 (12)	99 (15)		1 (10 per cent)
[O III] λ5007	5033.3 (0.002)	1588 (0.1)	22 (0.1)		−584 (1 per cent)
Hα (absorption)	6580.8 (0.16)	823 (7)	91 (08)	− 0.01	6 (10 per cent)
Hα (narrow)	6597.8 (0.02)	1599 (1)	17 (01)	0.77	−530 (3 per cent)
Hα (broad)	6598.2 (0.2)	1620 (9)	394 (10)	0.20	−136 (3 per cent)
Hα (red wing)	6617.7	2510	172	0.04	−29
Ca II λ8498	8542.6 (0.2)	1575 (5)	30 (6)		0.7 (17 per cent)
Ca II λ8542	8587.7 (0.3)	1604 (10)	26 (10)		0.4 (12 per cent)
Ca II λ8662	8707.7 (0.1)	1577 (3)	24 (3)		0.7 (13 per cent)

2013). It gives for the PHL 293B *Chandra* observation of 7.7 ks a point source sensitivity of about 3.5×10^{-15} erg cm^{-2} s^{-1}.

4 ANALYSIS

4.1 Ionizing cluster age, mass and abundance

PHL 293B is a low-luminosity ($M_B = -14.37$; Cairós et al. 2001), low-metallicity [12+log(O/H) = 7.61; Izotov et al. 2007 BCG. The comparison of our measured narrow Hα to Hβ flux ratio with the case B recombination theoretical value yields a logarithmic extinction at Hβ of c(Hβ) = 0.12. For our SDSS flux measurements and the assumed distance of 23.1 Mpc (NED) this gives an extinction corrected Hβ luminosity of 1.3×10^{39} erg s^{-1}. The total Lyman continuum photon rate for a given region can be derived from the Hα luminosity (e.g. Leitherer & Heckman 1995):

$$N(\mathrm{Lyc}) = 7.35 \times 10^{11} L(\mathrm{H}\alpha) = 2.71 \times 10^{51}\ \mathrm{s}^{-1}.$$

Taking into account that the number of Lyman continuum photons per unit mass of the ionizing population decreases with age, and using the equivalent width of Hβ (EW(Hβ)) as an age parameter (Dottori 1981), it is possible to calculate the mass of the ionizing star cluster under certain assumptions about the initial mass function (IMF). For a Salpeter IMF with lower and upper mass limits of 0.8 and 120 M$_\odot$, respectively, we have (Díaz et al. 2000)

$$\log[N(\mathrm{Lyc})/M_{\mathrm{ion}}] = 44.48 + 0.86 \log[|\mathrm{EW(H}\beta)|],$$

where the vertical bars indicates modulus.

For an EW(Hβ) = −100 Å, which represents the total EW of Hβ (see Table 1), the resulting ionizing star cluster mass is $M_{\mathrm{ion}} = 1.66 \times 10^5$ M$_\odot$.

According to the models of Mollá, García-Vargas & Bressan (2009), an EW(Hβ) = −100 Å may be produced by a cluster of 3.43×10^5 M$_\odot$ with an age of about 7×10^6 yr, for a metallicity of $Z = 0.0004$ or a cluster of 2.06×10^5 M$_\odot$ with an age of about 5×10^6 yr, for a metallicity of $Z = 0.004$. The ionized gas metallicity of PHL 293B is about $Z = 0.002$, i.e. in between the values of the

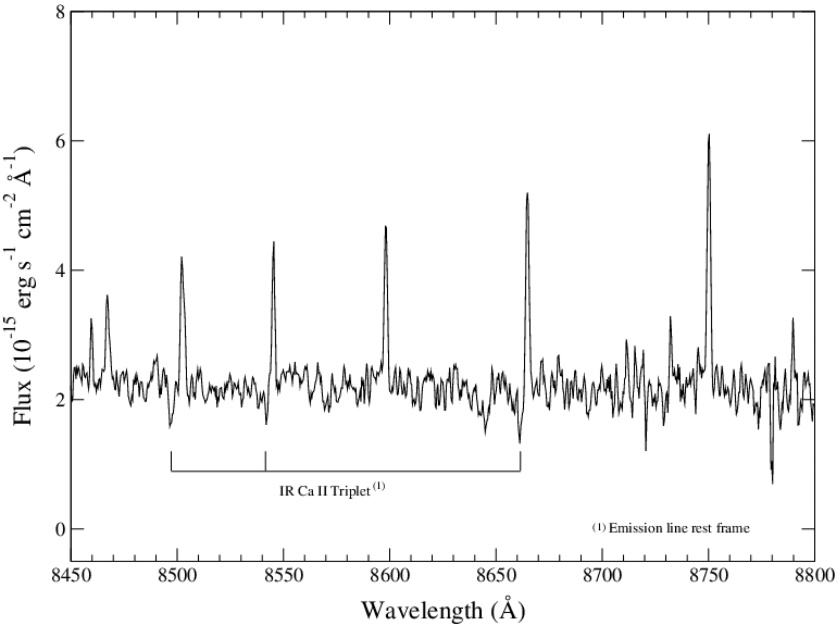

Figure 6. Visible NIR range of the X-shooter spectrum showing the emission lines from the Paschen series and the IR CaT stellar absorptions.

two models quoted, hence intermediate values for the mass of the ionizing cluster and the age can be expected. The observed EW may be affected by the continuum of an underlying older stellar population or a bright stellar component like for example an SN or an LBV; therefore, it has to be considered as a lower limit for the EW of the ionizing cluster, and our mass and age estimates are in consequence upper limits.

4.2 CaT lines

The IR CaT at nominal λλ8498, 8542 and 8662 Å is clearly seen in absorption in the spectrum of PHL 293B (see Fig. 6) at the same redshift shown by the narrow emission lines. The CaT index definition (Díaz, Terlevich & Terlevich 1989; Terlevich, Díaz & Terlevich 1990) that uses the two strongest lines of the triplet, measures approximately 2 Å, which, if taken literally, suggests [Fe/H] < -2.0 for giant or supergiant stars (see e.g. Díaz et al. 1989). This index has to be corrected for the contribution of the nebular continuum. For the model of log(age) $= 6.86$ and $Z = 0.0004$ chosen above, this contribution amounts to 0.55 Å per line and hence the corrected CaT index would be 3.1 Å, consistent with the values calculated by García-Vargas, Mollá & Bressan (1998) from single stellar population synthesis models for the lowest abundance they consider, $Z = 0.004$.

For the assumed mass, age and metallicity of the ionizing cluster the models by Mollá et al. (2009) predict no WR stars and only one or two red supergiant (RSG) stars.

4.3 Ionized gas mass

PHL 293B is unusual as an H II galaxy due to the presence of broad permitted and narrow forbidden lines in its optical spectrum. The absence of a strong broad forbidden [O III] λ5007 component indicates that the density of the gas producing the broad component is high enough to collisionally de-excite [O III] λ5007 (a condition for which the electron density has to be $N_e \geq 10^8$ cm^{-3}). An upper limit to the mass of the ionized gas in the broad line region can be estimated using the observed $L(\mathrm{H}\alpha)$ (Macchetto et al. 1990) and the electron density lower limit,

$$M(\mathrm{H\,II}) = 3.32 \times 10^{-33} L(\mathrm{H}\alpha)/N_e,$$

therefore,

$$M(\mathrm{H\,II})_{\mathrm{broad\ comp}} \lesssim 3 \times 10^{-2}\,\mathrm{M}_\odot.$$

The ionized gas mass of the narrow line region is, assuming an electron density of 100 cm^{-3} (derived from the [S II] doublet ratio in our ISIS data),

$$M(\mathrm{H\,II})_{\mathrm{narrow\ comp}} \sim 1.22 \times 10^5\,\mathrm{M}_\odot,$$

similar to the ionizing star cluster mass determined in Section 4.1.

4.4 Photometric variability (or lack of it)

From the nightly averaged data (pluses) in Fig. 8 no variability is detected. Dividing the data into nine groups of one year duration each (filled diamonds in the same figure) reduces the rms scatter to 0.009 per group as expected for a non-variable sample and again no systematic trend in the luminosity is apparent; furthermore a cursory analysis indicates that there is no periodic variation.

Based on the CSS data we can infer that at 3σ level any long-term variability, i.e. over a few years, cannot be larger than 0.02 mag and that any medium term variability, i.e. over a few months, should be less than 0.04 mag. Further still, including the data from Cairós et al. (2001), Kinman (1965) and SDSS, we can safely conclude that there is no variability at the level of few tenths of magnitude over a period of 25 yr.

5 DISCUSSION

5.1 P Cygni profiles

To generate relatively narrow P Cygni-like absorption profiles such as the ones observed in PHL 293B, the absorbing material must cover a substantial fraction of the continuum source, in this case a

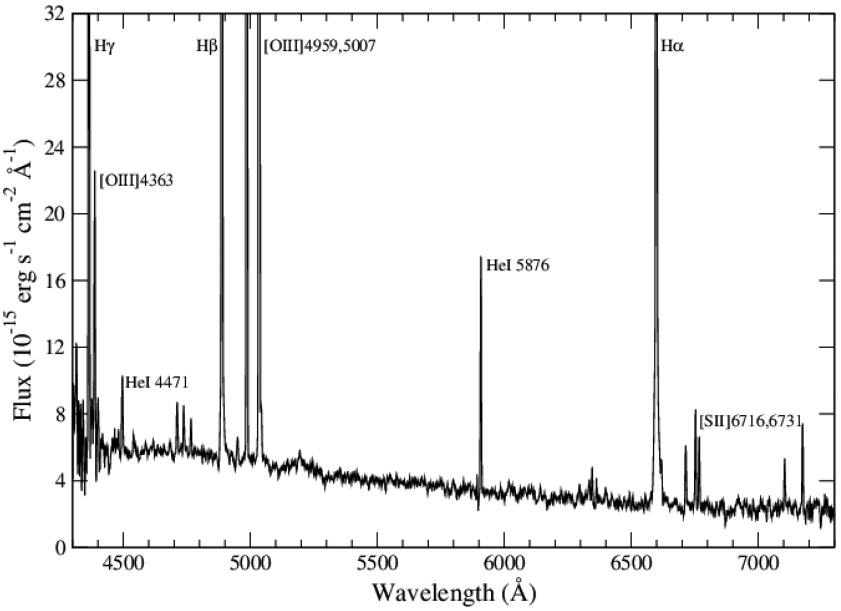

Figure 7. WHT-ISIS spectrum box smoothed by 5 pixels.

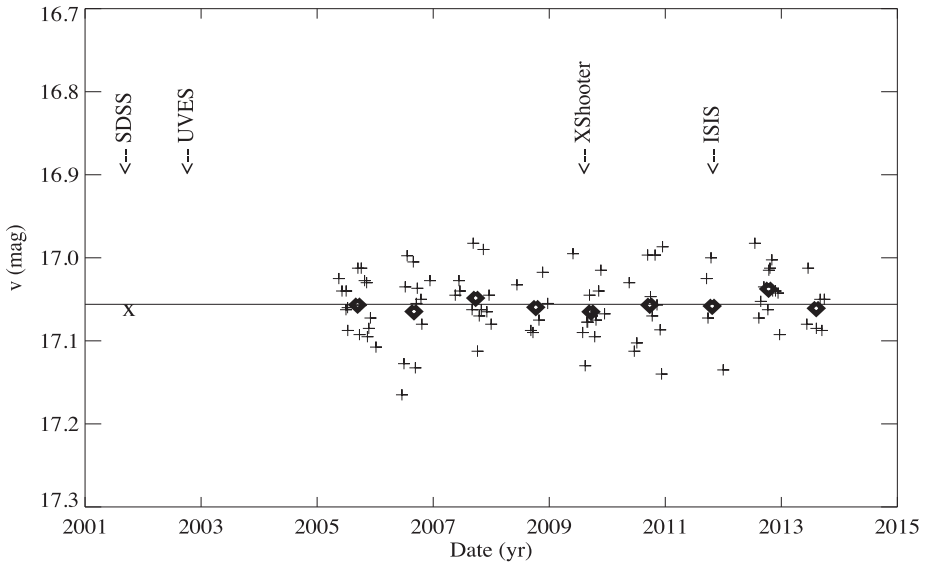

Figure 8. PHL 293B CSS photometry from 2005 April to 2013 October. There are 353 observations in 91 observing nights. Most night results are made out of four independent observations. The average night magnitude is plotted with a plus sign. The nine filled rhomboids are the yearly averages. The horizontal line represents the average magnitude 17.056 ± 0.004. The x indicates the SDSS Petrosian *g* magnitude converted to *v* magnitudes. For older photometry see text. The labelled arrows show the dates corresponding to the spectroscopy.

young stellar cluster several parsecs in size. These absorptions may be produced in an expanding dense supershell created by the interaction of combined stellar winds with the circumcluster medium (CCM). An expanding supershell has been postulated to explain the blueshifted metal absorption detected in the UV spectrum of several nearby and high-redshift H II galaxies (Tenorio-Tagle et al. 1999; Mas-Hesse et al. 2003).

Alternatively, the observed blueshifted narrow absorptions could be associated with a single star in a very luminous transient phase like an LBV or an SN IIn.

5.2 P Cygni profiles and the He I lines

The possibility that the P Cygni-like profiles in PHL 293B are originated in the powerful wind of an LBV has been extensively discussed by Izotov et al. (2011). These authors suggested that the absorptions seen at λ4939 and λ5031 Å are in fact the blueshifted absorptions associated with the He I lines at rest wavelengths λ4921 and λ5016 Å in accordance with the P Cygni profile of the Balmer lines.

Fig. 9 shows the spectral regions around the He I optical lines from the X-shooter data. The dotted line corresponds to a blueshift

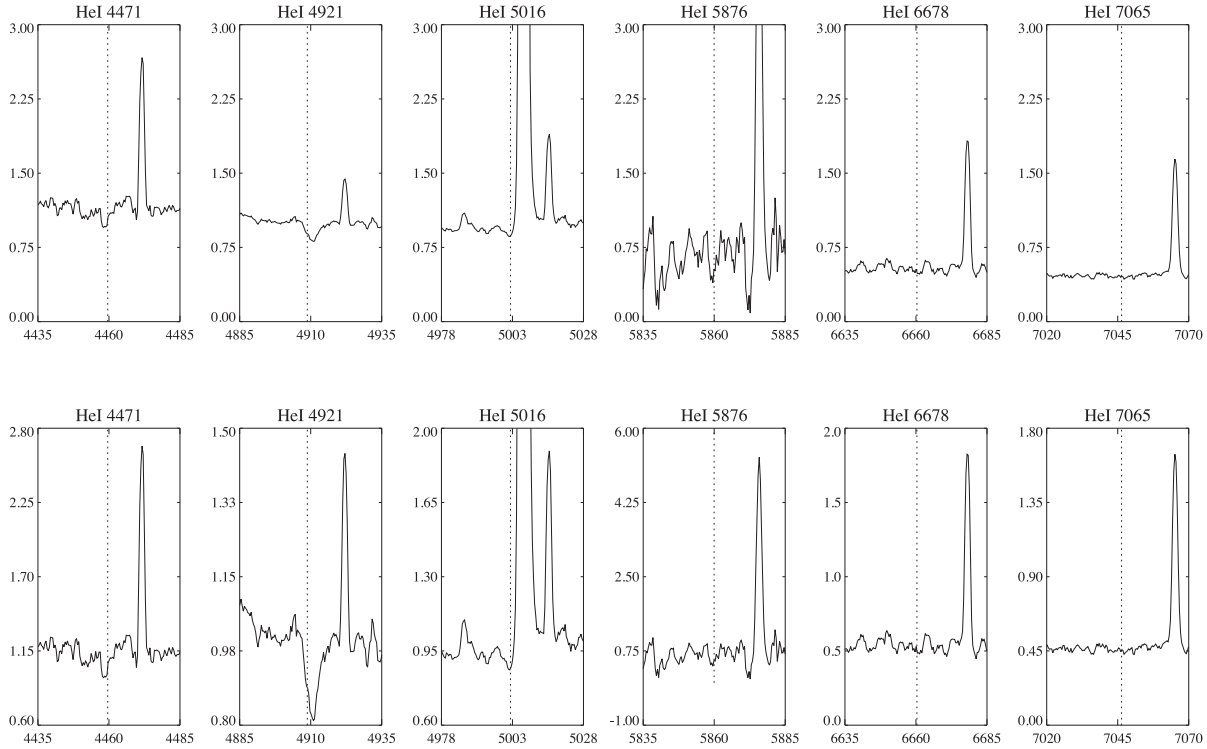

Figure 9. Spectral regions around the He I optical lines from the X-shooter data. The dotted line corresponds to a blueshift of 800 km s^{-1}. Top row spectra are plotted with the same scale in flux to show the relative importance of the emissions. Bottom row shows the spectra normalized to the same amplitude for the emission line and the continuum to illustrate the differences in the associated absorptions. See text regarding the strong absorption to the blue of He I λ4921 Å, shifted with respect to the 800 km s^{-1} line.

of 800 km s^{-1} consistent with what is observed in the Balmer lines. The top row displays all the He I lines with the same flux scale in order to show the relative importance of the emissions. The bottom row shows the spectra normalized to the same amplitude for the emission line and the continuum to illustrate the differences in strength of the associated absorptions.

It is clear that while the He I λ4921 Å emission is the weakest, the absorption to the blue is the strongest and furthermore it is redshifted with respect to the 800 km s^{-1} line. Izotov et al. (2011) attributed this difference in velocity between Balmer and He I lines' P Cygni-like profiles to the different formation depth of the core of each line in an accelerated wind. However, there are several difficulties with this suggestion. First, the broad absorption to the blue of He I λ4921 Å has an EW similar to that of the P Cygni-like absorption of Hβ, probably too large to be associated with such a weak He I line. Secondly, it is not clear why much stronger He I lines like λλ5876, 6678 and 7065 Å do not show a blueshifted absorption as can be seen in Fig. 9, although He I 5876 Å seems to have, at the noise level, an associated weak absorption.

5.3 The absorption lines of Fe II multiplet 42

An important clue for an alternative interpretation of the absorptions seen at λ4939 and λ5031 Å is given by the discovery of a previously unidentified absorption at λ ∼5183 Å (Fig. 3) corresponding to λ5155 Å in the rest frame of the forbidden lines and λ5169 Å in the rest frame of the blueshifted Balmer absorptions. This absorption is real and is present in the spectra from SDSS, VLT-UVES, VLT-X-shooter and WHT-ISIS that were taken in four different epochs (see Fig. 10). Although the λ ∼5183 Å absorption could be attributed to Mg2 λ5172 Å present in late star spectra, this possibility can be readily dismissed given that the observed wavelength would imply a shift of 1050 km s^{-1}with respect to the galaxy rest frame and definitely inconsistent with the presence of the CaT lines at the galaxy velocity rest frame.

A more plausible interpretation is that we are in fact detecting the Fe II multiplet (42) λλ4923.93, 5018.44 and 5169.03 Å blueshifted by the same amount as the Balmer absorption features i.e. ∼800 km s^{-1} to λλ4911, 5005 and 5155 Å. These absorptions have already been detected in a variety of transient luminous objects like the LBV candidate NGC 2366-V1 or SNe IIn like 1995G, 1999el or 1999eb among others (see fig. 2 of Di Carlo et al. 2002).

LBVs represent a short (∼10^4 yr) phase in the evolution of massive stars during which the star undergoes luminous outbursts associated with large mass-loss events. During these short phases lasting few years the LBV can reach, in extreme cases, 10^6 L$_\odot$ or Mv ∼ −10 and luminosity variations of ∼1 mag. The luminosity changes are in general correlated with spectral changes. The typical absolute magnitude of an LBV in quiescent state is Mv ∼ −6. In general, information about LBVs is very sparse given that only 35 candidates have been identified in our galaxy (Clark, Larionov & Arkharov 2005). Only two of these, η Car and P Cygni, were observed during an outburst. Extragalactic examples are known due to either photometric or specific spectral variability. The mechanism responsible for the outbursts remains unidentified.

It is important to mention that the wind terminal velocities quoted by Izotov et al. (2011, 700–850 km s^{-1}) are significantly larger than the usual range for LBVs (100–250 km s^{-1} up to 500 km s^{-1} for η Car; Leitherer et al. 1994). This discrepancy is attributed by Izotov et al. to the very low metallicity of PHL 293B.

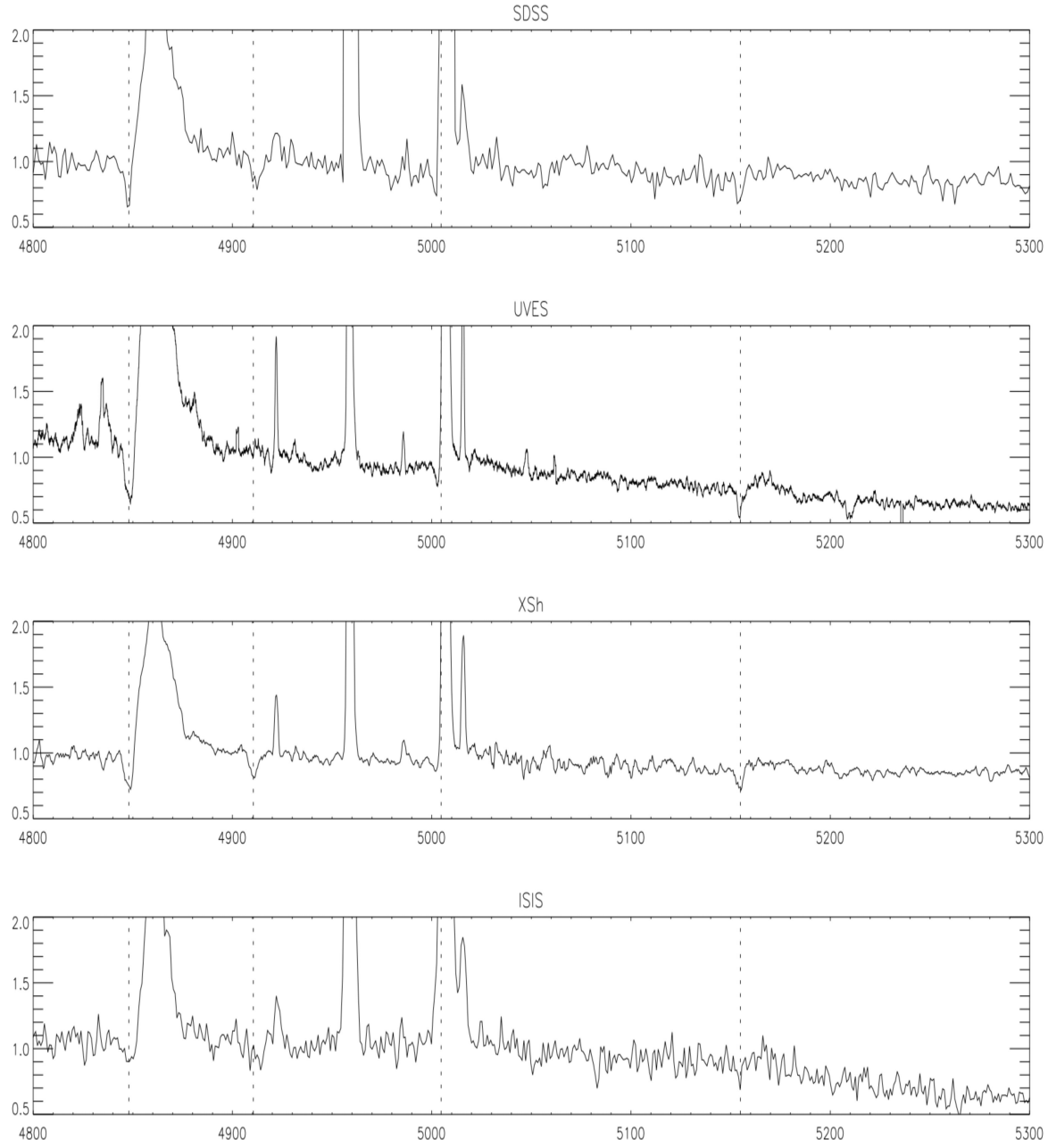

Figure 10. The four panels show the SDSS, VLT-UVES, VLT-X-shooter and WHT-ISIS data in the range 4800–5300 Å. The position of the Hβ and the Fe II(42) multiplet absorptions, all blueshifted by 800 km s^{-1}, are indicated with dotted lines.

There are two striking examples of LBVs in low-metallicity dwarf galaxies, one in NGC 2366 and the other one in IC1613.

NGC 2366 is a giant H II region (similar to 30 Dor in the LMC) located in the metal poor (12+log(O/H) = 7.9, i.e. O/H ∼ 0.16 solar; González-Delgado et al. 1994) dwarf galaxy NGC 2363, a member of the M81 group. The variable star NGC 2366-V1 showed a big eruption similar to an LBV with an amplitude of 3.5 mag in 4 yr reaching a maximum of about Mv = −10.2 (Drissen, Roy & Robert 1997). After the outburst it started a decline of about 0.25 mag in 6 yr accompanied by ∼0.2 mag dips lasting about a year each. Regarding its spectral evolution, the Fe II lines (4923, 5018 and 5171) present between 1997 and 2000 disappeared later while the He I transited from absorption to emission and the P Cygni feature in Hα disappeared (Petit, Drissen & Crowther 2006). These authors reported an average wind terminal velocity of ∼300 km s^{-1} for NGC 2366-V1.

IC 1613 is a dwarf irregular galaxy in the Local Group with a metallicity of log(O/H)+12 = 7.80 ± 0.10 as determined from its B-supergiants (Bresolin et al. 2007). Nebular abundance estimates vary between 7.60 and 7.90 (Lee, Grebel & Hodge 2003), similar to the metallicity values shown by NGC 2363 and PHL 293B.

The peculiar variable star V39 (Sandage 1971) was studied in detail by Herrero et al. (2010). Its spectrum shows strong Balmer and Fe II P Cygni profiles combined with weak He I emission similar to the early stages of the evolution of the NGC 2366-V1 LBV star. The EW of the Hα P Cygni profile was ∼45 Å in emission and ∼2.3 Å in absorption with a blueshift or wind terminal velocity of ∼400 km s^{-1}. Its absolute magnitude reached Mv = −8.1.

Table 3. X-shooter, UVES, SDSS and ISIS EW of absorption lines of Hβ , components 1 and 3 of the Fe II(42) multiplet and [O III] λ4959 Å. Measurements are in the galaxy rest frame. Flux in units of 10^{-17} erg s^{-1}.

Spectra	Hβ			Fe II(42) 1			Fe II(42) 3			[O III]4959		
	Wav. (Å)	EW (Å)	Vr (km s^{-1})	Wav. (Å)	EW (Å)	Vr (km s^{-1})	Wav. (Å)	EW (Å)	Vr (km s^{-1})	Wav. (Å)	Flux	EW (Å)
SDSS	4847.3	1.1	−866.	4912.2	1.0	−715.	5154.5	0.67	−843.	4959.1	164	−171.
UVES	4848.1	2.0	−816.	–	–	–	5154.7	0.88	−832.	4959.0	192	−208.
X-shooter	4848.0	1.1	−822.	4910.8	0.91	−800.	5154.5	0.68	−843.	4959.0	186	−197.
ISIS	4847.9	1.0	−829.	4912.0	0.71	−727	5154.7	0.57	−832.	4959.1	220	−211.

The Fe II (42) absorptions in these two transient objects show EWs of about 2 Å while the observed value in the spectrum of PHL 293B is just under 1 Å. The contribution of the nebular continuum at the Fe II wavelengths is 25 per cent (see above), which increases this value to 1.3 Å. This implies that under this hypothesis, about 30 per cent of the observed continuum should be due to the transient object itself. But, the absolute magnitude of PHL 293B is Mv $= -14.5$ while a very luminous LBV during outburst would reach Mv ~ -10, thus contributing less than 2 per cent of the total luminosity i.e. more than one order of magnitude smaller than what is needed to explain the observed strength of the Fe II absorptions (see Table 3).

It seems important to notice that these two LBVs, both located in low-metallicity environments, show wind terminal velocities that are typical of LBV (100–250 km s^{-1}) while η Car, belonging to a region that is not metal poor ($12 + \log$ O/H $= 8.36 \pm 0.03$; Pilyugin, Ferrini & Shkvarun 2003), has a larger wind terminal velocity (up to 500 km s^{-1}).

Wind velocities between 100 and 1000 km s^{-1} are reported for transient events or 'supernova impostors' that could be related to powerful eruptions of LBVs (Smith et al. 2011), and in a very interesting recent work Koss et al. (2014) report an unusual variable source in the nearby dwarf galaxy MRK 177 (UGC 239) that they suggest can be explained as an LBV eruption followed by an SN IIn like event in 2001.

Nazé, Rauw & Hutsemékers (2012) discussed the X-ray properties of the Galactic LBVs. They found that their X-ray luminosities in the 0.5–8 keV range are between $\sim 8 \times 10^{29}$ and $\sim 4 \times 10^{34}$ erg s^{-1}. The estimated minimum luminosity for a point source to be detected in the ACIS-*Chandra* image of PHL 293B is about 2.2×10^{38} erg s^{-1} (see Section 3.2) about three orders of magnitude higher than the largest reported values for Galactic objects.

5.4 Lack of optical variability

One fact supporting the hypothesis of the presence of a transient object would be the detection of long-term variability in the flux from PHL 293B. However, as stated in Section 4.4, we can conclude that there is no variability at the level of a few hundredths of magnitude over 25 yr. This implies that any long-term variable component has to be fainter than $V = 21.5$. For a distance modulus $(m - M) = 31.8$, this upper limit means that any long-term variable component has to be fainter than $M_V = -10.5$. However, this does not exclude the possibility that we are observing such a transient object during a non-variable phase. The caveat in that case is that, if the variable component is that faint in relation with the ionizing cluster, it will be difficult to explain the observed strength of the Balmer and Fe II absorptions.

5.5 An old SN IIn?

An alternative scenario for the broad lines and pseudo P Cygni profiles in PHL 293B is that they are originated in an evolved SN IIn. It is usually assumed that SN IIn explode inside the circumstellar material previously ejected in the form of a slow dense wind by the red supergiant SN progenitor. What is observed is the result of the interaction between the ejecta and this slowly expanding dense circumstellar medium (CSM) which transforms the mechanical energy of the ejecta into radiation. These events are known as SN IIn or compact supernova remnants (see e.g. Chugai 1991; Terlevich et al. 1992; Filippenko 1997; Fassia et al. 2001; Chugai et al. 2004; Turatto 2005). In this interaction, radiative cooling can become catastrophic and these remnants rapidly radiate most of the mechanical energy in a relatively short time-scale and so they are highly luminous. The energy output is mostly in the extreme UV and X-ray regions of the spectrum. The optical continuum is a mixture of young stars and the emission from the SN IIn with fast moving high-density gas producing the broad line emission.

The spectra of some SNe IIn associated with H II regions like 1995G, 1999el or 1999eb among others, present broad Balmer components with relatively narrow P Cygni-like absorptions plus narrowish Fe II absorption with multiplet (42) being the strongest (see fig. 2 of Di Carlo et al. 2002). A significant constraint on the SN IIn/compact remnant scenario is the long-term lack of variability in PHL 293B. The secular variability of the broad lines in this scenario comes from the evolution of the interaction of the ejecta and the CSM, i.e. the evolution of the compact remnant. The evolution of the blue light-curve can be parametrized as $L_B \propto t^{-11/7}$ (Aretxaga & Terlevich 1994; Aretxaga, Cid Fernandes & Terlevich 1997) with its peak luminosity being a function of the circumstellar density ($L_B{}^{peak} \propto n^{3/4}$). These are analytical approximations and their predicted values should be taken as such.

We note that the observed absolute magnitude of PHL 293B (~ -14.8) is fainter than the absolute magnitude of a single compact remnant near peak (~ -15.5 for $n \sim 10^4$ cm^{-3}). This, together with the upper limit for the rate of change for the last ~ 30 yr, is only consistent with the very late stages of the evolution of a compact remnant, i.e. when its light curve flattens. Using the $t^{-11/7}$ time dependence of the luminosity as an indicator, we find that a compact remnant of age ~ 150 yr evolving in a medium with density $n \sim 10^4$ cm^{-3} would have shown a decline of about 1.5 mag since maximum and of about 0.1 mag in the last 10 yr.

We can estimate its line luminosities using the models of Terlevich et al. (1992). The observed luminosity of the broad component of Hα is

$$L_{H\alpha} \sim 10^{39} \text{erg s}^{-1} .$$

From the analytical solutions of Terlevich et al. (1992) and tables 1.1 and 1.2 of Terlevich (1994) it is possible to estimate that a

compact remnant evolving in a medium with $n \sim 10^4$ cm^{-3} would have a shock velocity of 800 km s^{-1} at an age defined by t_{sg} of about 112 yr. Predicted values for the shock parameters and Hα corresponding to such age are

$T_{\rm Sh} \sim 1 \times 10^7$ K

$L_{\rm Sh} \sim 1 \times 10^{41}$erg s^{-1}

$L_{\rm H\alpha} \sim 3 \times 10^{39}$erg s^{-1}

$R_{\rm Sh} \sim 0.3$ pc

$n_{\rm Sh} \sim 4 \times 10^7$ cm^{-3}

and the FWZI of the broad component is about twice the shock velocity or 1600 km s^{-1}. Given its temperature, the remnant is expected to emit in X-rays up to about few keV with a luminosity just below $\sim 10^{41}$erg s^{-1}. These values are too large compared with the observed upper limit of $\sim 2.2 \times 10^{38}$erg s^{-1}. Furthermore, the expected drop in luminosity 7.5 yr later i.e. at an age of 119.5 yr is 10 per cent or about 0.1 mag and the drop in luminosity in 20 yr is about 0.2 mag; thus, we can safely conclude that the observed upper limit on the variability of PHL 293B makes it very difficult for the observed absorptions and broad emission to be originated in an SN IIn.

In summary, we have evidence that an old compact remnant could explain the observed broad lines and the dense shell responsible for the blueshifted absorptions in PHL 293B. But, while the observed line properties are in rough agreement with a compact remnant slightly older than 100 yr, this age is much smaller than the age derived from the absolute blue magnitude limit imposed by the lack of variability and furthermore the expected variability in Hα at 100 yr is also too large compared with the limits deduced from the data.

5.6 Spectral variability (or lack of it)

To see if there is some information in the data regarding the spatial distribution of the absorbers, we compared in Table 3 the EW measurements of the hydrogen absorptions that are supposed to cover most of the source of the continuum, with the ones of the Fe II lines taking as reference the EW of [O III] λ5007 that is expected to extend beyond most of the ionizing cluster continuum but to be still inside the host galaxy continuum.

The EW of the Hβ and Fe II absorptions are, within errors, basically the same in all four sets of data.

To check for aperture effects, we measured the EW of [O III] λ5007 and the results are displayed in Table 3. As expected, there is a slight increase in the EW measured with the smaller X-shooter aperture (1 arcsec) compared with the 3 arcsec circular aperture of the SDSS spectrum (although determination of faint continuum contribution can also account for such variations among spectra).

We have also checked for possible variability in the broad emission components. The broad and narrow components of Hα are listed in Tables 1 and 2. Their ratio of the broad to total Hα flux is, for both SDSS and X-shooter observations, the same within errors, about 0.21 showing no indication of variability as already discussed.

5.7 The expanding supershell and stationary cooling wind scenarios

The lack of variability imposes a strong constraint for scenarios involving discrete transient sources like LBVs or SNe IIn. At the same time the lack of variability suggests that the origin of the blueshifted absorptions could be associated with a global process involving a large part of the ionizing cluster. Furthermore, we have to address the fact that what we are witnessing in the Fe II lines and perhaps also in the Balmer series in PHL 293B are blueshifted absorptions without the associated narrow emissions typical of classical P Cygni profiles. This lack of associated emissions indicates that the material responsible for the detected absorptions, while covering a large part of the continuum source, is not an extended CCM. If it was it would have produced the so far undetected associated emission lines.

Luminous regions of star formation in the nearby universe like Orion or NGC 3606 in our galaxy, 30-Doradus in the LMC or NGC 604 in M33, to name just a few of the nearest ones, all show gaseous filaments surrounding the ionizing cluster. This fact and the observed lack of variability over many years suggest a scenario where the blueshifted absorptions found in PHL 293B are formed in an expanding supershell generated by the cluster wind interacting with a moderately dense gas closely surrounding the SFR. The cluster wind drives a shock into the CCM and a recombined dense shell is formed in the post-shock region. This dense shell expanding at 800 km s^{-1} produces the observed blueshifted absorptions in H and Fe following catastrophic radiative cooling in a scenario similar to the case of the compact supernova remnant described above. The main difference being that instead of an instantaneous input of energy and mass the wind scenario involves a constant rate. As the cluster wind shocks the surrounding ISM it will generate, given adequate conditions, a post-shock high-density supershell that will be ionized by the cluster UV output modified by the radiative shock emission.

As already mentioned, a supershell scenario has been postulated to explain the diversity of Lyα profiles observed in starbursts (see Tenorio-Tagle et al. 1999; Mas-Hesse et al. 2003, and references therein) where also blueshifted UV ISM metal absorption lines are observed. In this scenario, the Lyα emission and the blueshifted metal absorption lines are formed in an expanding supershell generated by the interaction of the combined stellar winds and supernova ejecta from the young starburst, with an extended gaseous halo.

Among the many intrinsic parameters of an SFR that can affect the properties of the observed emission line profiles, velocity, density and ionization distributions of the gas along the line of sight are by far the dominant ones. The expulsion of dust and gas from young clusters due to the action of stellar winds and supernovae has been discussed by many authors (see for example Tutukov 1978; Bastian & Goodwin 2006; Goodwin & Bastian 2006) as well as the resultant cluster 'infant mortality' effect (see for example Grosbøl & Dottori 2013).

The strength of a weak absorption line depends on its oscillator strength f, its wavelength λ and column density N. If the element is mostly in one ion state and there is no line saturation the relation between the column density N and the EW$_\lambda$ is given by Morton (1991):

$$\log(N) = \log({\rm EW}_\lambda/\lambda) - \log(\lambda f) + 20.053.$$

From the X-shooter spectra of PHL 293B, we have measured EW = 0.91 and 0.68 Å for the Fe II lines 4923 and 5169 Å, respectively. The corresponding oscillator strengths are 0.0104 and 0.0226 (Giridhar & Arellano Ferro 1995; Kramida et al. 2012). With these values for the oscillator strength we can compute the Fe$^+$ column density,

$N_{\rm Fe^+} \sim 4.1 \times 10^{14}$ cm^{-2}

and

$$N_{\mathrm{Fe^+}} \sim 1.4 \times 10^{14}\,\mathrm{cm^{-2}}$$

for the Fe II lines 4923 and 5169 Å, respectively. The Fe^+ column density values are in good agreement with each other within observational errors.

If the supershell is formed from shocked CCM, it must have abundances similar to those observed in the ionized gas. If Fe/O is solar, this implies for the supershell Fe/H $\sim 3 \times 10^{-6}$ and therefore the hydrogen column density associated with Fe^+ is

$$N_{\mathrm{H^+}} \sim 10^{20}\,\mathrm{cm^{-2}}$$

or

$$N_{\mathrm{H^+}} \sim 2 \times 10^{20}\,\mathrm{cm^{-2}}$$

if Fe/O is half solar. Given that we do not know the hydrogen ionization fraction, these values should be taken as an estimate of the total, i.e. neutral plus ionized, hydrogen column density.

Following the same procedure, we can estimate from the Balmer absorptions the column density of neutral hydrogen. For a measured EW = 6 and 2 Å for Hα and Hβ the column density estimates of neutral hydrogen are, respectively,

$$N_{\mathrm{H}} \sim 3 \times 10^{13}\,\mathrm{cm^{-2}}$$

and

$$N_{\mathrm{H}} \sim 8 \times 10^{13}\,\mathrm{cm^{-2}}.$$

The comparison of the column density of 'total' and neutral hydrogen suggests a high degree of ionization in the gas that is producing the blueshifted absorptions.

An interesting variant of this scenario is provided by the Super Star Cluster cooling wind model of Silich, Tenorio-Tagle & Rodríguez-González (2004), Tenorio-Tagle et al. (2007) and collaborators. This group has shown that in the case of a very massive and extremely compact young cluster its wind may radiatively cool in a stationary condition close to the outer radius of the cluster. This cool ejecta should be the responsible agent for the broad emission and blueshifted absorptions observed (see fig. 4a of Tenorio-Tagle et al. 2007). We expect to see soon detailed model calculations for the supershell and stationary cooling wind scenarios and the comparison of the theoretical predictions with the observed parameters of PHL 293B.

If the Fe II absorptions are formed in a stationary cooling wind, the metal abundances will be those of the combined ejecta of stellar winds and SNe. In this scenario, Fe/H will be much higher than that of the ISM in PHL 293B and consequently the estimated $N_{\mathrm{H^+}}$ column density will be proportionally lower than those estimated above. Assuming solar abundances for the cluster wind, the estimated ionized hydrogen column density will be

$$N_{\mathrm{H^+}} \sim 10^{19}\,\mathrm{cm^{-2}}.$$

A question that is raised in these relatively long-lived cluster wind scenarios is: Why is it that among several thousand H II galaxies known, only PHL 293B is known to have simultaneously narrow blueshifted Balmer and Fe II absorptions? or equivalently, Why is this type of event so rare?

The answer may be related to the fact that we are witnessing an event that produces weak narrow absorptions that are detectable only with high-dispersion and high-S/N spectra.

6 CONCLUSIONS

We have analysed spectra of the low-metallicity star-forming galaxy PHL 293B corresponding to four epochs obtained in four different combinations of telescopes and spectrographs, the SDSS, VLT-UVES, VLT-X-shooter and WHT-ISIS.

We find moderate narrow absorption components in the Balmer series blueshifted by 800 km s^{-1}. We detected also the IR CaT lines at the galaxy velocity rest frame, i.e. the rest frame defined by the ionized gas narrow emission lines. We also find narrow absorptions at $\lambda \sim 4911$ Å, at $\lambda \sim 5004$ Å (partially filled up by [O III] λ5007 Å) and a previously unidentified absorption at $\lambda \sim 5183$ Å. We interpret these narrow absorptions as the Fe II multiplet (42) $\lambda\lambda$4923.93, 5018.44 and 5169.03 Å, similar to those detected in a variety of transient luminous objects like the LBV candidate NGC 2366-V1 or SNe IIn 1995G, 1999el or 1999eb, blueshifted by the same amount as the Balmer absorption features, i.e. $\sim$800 km s^{-1} to $\lambda\lambda$4911, 5005 and 5155 Å.

The analysis of the photometric data provided by the CSS puts a strong upper limit to the possible variability of PHL 293B. Basically, any optical yearly variability allowed by the data should be smaller than 0.02 mag at the 3σ level in the 8.5 yr between 2005 April and 2013 September. The possibility of any secular trend in the luminosity of PHL 293B in the last 15 yr (considering only CCD data) is also limited to at most 0.02 mag at the 3σ level.

This lack of variability and the observed strength of the Balmer and Fe II absorptions rule out any transient of the type of an LBV or SN IIn as the origin of the blueshifted absorptions of H and Fe II.

The evidence points to either a young and dense expanding supershell or a stationary cooling wind, both driven by the young cluster wind. We suggest that the observed absorptions and broad Balmer emissions are originated in one of these scenarios which seem capable of explaining the observed spectral features, the constant (within errors) photometric history and the rarity of the phenomenon.

Many starbursts, both nearby and at high z, show blueshifted far-UV ISM narrow absorption lines. On that basis, coupled with the observational evidence, we expect that the far-UV spectrum of PHL 293B will show blueshifted ISM lines and moderate Lyα emission with perhaps a P Cygni-like profile.

We have to bear in mind that there are not many H II galaxies known to show prominent broad wings in their emission lines and none with the quality of the data presented here for PHL 293B. This leaves open the possibility that we are witnessing an event not detected in other systems due to low-S/N data. Even if it is true that we haven't been actively looking for them, and that data of the quality and variety discussed here are not widely available, it is still puzzling that Fe absorptions have not been detected in other star-forming H II galaxies. A search should be performed in high-dispersion, high-signal-to-noise spectra of H II galaxies to investigate the presence of supershells in starbursts with or without strong broad components in the Balmer lines. Until such data are gathered and analysed, the fact that we do not see many H II galaxies showing spectra similar to PHL 293B means that this may be a relatively short duration stage in the evolution of compact and massive stellar clusters, lasting perhaps only a few thousand years.

ACKNOWLEDGEMENTS

ET and RT are grateful to the Mexican Research Council (CONACYT) for support under grants 2008-103365 and 2010-01-155046. Financial support for this work has also been provided by the Spanish *Ministerios de Educación y Ciencia and Ciencia e Innovación*

under grants AYA2007-67965-C03-03 and AYA2010-21887-C04-03. VF acknowledges support from ESO-Chile Joint Committee and DIULS. Our team enjoyed the hospitality of the Institute of Astronomy, Cambridge, of the Departamento de Física Teórica of the Universidad Autónoma de Madrid and of the Observatorio Astronómico of the Universidad Nacional de La Plata (Argentina) during fruitful visits when this paper was started and developed. We thank Vahram Chavushyan for suggesting the identification of the Fe II absorption features in λλ4911, 5155 Å and discussions with Daniel Kunth helped to clarify the estimates of the analysis of these Fe II features. Greatly enjoyed were discussions with Guillermo Tenorio-Tagle, Sergiy Silich and Sergio Martínez-González, from which a picture of the stationary wind scenario started to emerge. We are grateful to Vital Fernández for helping with the reduction of the WHT data. We thank the X-shooter data reduction team for valuable help and suggestions and an anonymous referee whose questionings greatly improved the clarity of the paper.

The CSS survey is funded by the National Aeronautics and Space Administration under Grant No. NNG05GF22G issued through the Science Mission Directorate Near-Earth Objects Observations Program. The CRTS survey is supported by the US National Science Foundation under grants AST-0909182. This research has made use of NED which is operated by the Jet Propulsion Laboratory, California Institute of Technology, under contract with the National Aeronautics and Space Administration.

REFERENCES

Abazajian K. N. et al., 2009, ApJS, 182, 543
Aretxaga I., Terlevich R., 1994, MNRAS, 269, 462
Aretxaga I., Cid Fernandes R., Terlevich R., 1997, MNRAS, 286, 271
Aretxaga I., Benetti S., Terlevich R. J., Fabian A. C., Cappellaro E., Turatto M., della Valle M., 1999, MNRAS, 309, 343
Asplund M., Grevesse N., Sauval A. J., Scott P., 2009, ARA&A, 47, 481
Bastian N., Goodwin S. P., 2006, MNRAS, 369, L9
Bresolin F., Urbaneja M. A., Gieren W., Pietrzyński G., Kudritzki R.-P., 2007, ApJ, 671, 2028
Cairós L. M., Vílchez J. M., González Pérez J. N., Iglesias-Páramo J., Caon N., 2001, ApJS, 133, 321
Castañeda H. O., Vilchez J. M., Copetti M. V. F., 1990, ApJ, 365, 164
Chugai N. N., 1991, MNRAS, 250, 513
Chugai N. N., Blinnikov S. I., Cumming R. J., Lundqvist P., Bragaglia A., Filippenko A. V., Leonard D. C., Matheson T., 2004, MNRAS, 352, 1213
Clark J. S., Larionov V. M., Arkharov A., 2005, A&A, 435, 239
Di Carlo E. et al., 2002, ApJ, 573, 144
Díaz A. I., Terlevich E., Pagel B. E. J., Vilchez J. M., Edmunds M. G., 1987, MNRAS, 226, 19
Díaz A. I., Terlevich E., Terlevich R., 1989, MNRAS, 239, 325
Díaz A. I., Castellanos M., Terlevich E., Luisa García-Vargas M., 2000, MNRAS, 318, 462
Dottori H. A., 1981, Ap&SS, 80, 267
Drake A. J. et al., 2009, ApJ, 696, 870
Drissen L., Roy J.-R., Robert C., 1997, ApJ, 474, L35
Fassia A. et al., 2001, MNRAS, 325, 907
Filippenko A. V., 1997, ARA&A, 35, 309
French H. B., 1980, ApJ, 240, 41
García-Vargas M. L., Mollá M., Bressan A., 1998, A&AS, 130, 513
Geha M., Blanton M. R., Masjedi M., West A. A., 2006, ApJ, 653, 240
Giridhar S., Arellano Ferro A., 1995, Rev. Mex. Astron. Astrofis., 31, 23
González-Delgado R. M. et al., 1994, ApJ, 437, 239
Goodwin S. P., Bastian N., 2006, MNRAS, 373, 752
Grosbøl P., Dottori H., 2013, A&A, 551, L13
Haro G., Luyten W. J., 1962, Bol. Inst. Tonantzintla, 3, 37
Herrero A., Garcia1 M., Uytterhoeven K., Najarro F., Lennon D. J., Vink J. S., Castro N., 2010, A&A, 513, A70
Izotov Y. I., Thuan T. X., 2009, ApJ, 690, 1797
Izotov Y. I., Dyak A. B., Chaffee F. H., Foltz C. B., Kniazev A. Y., Lipovetsky V. A., 1996, ApJ, 458, 524
Izotov Y. I., Thuan T. X., Stasińska G., 2007, ApJ, 662, 15
Izotov Y. I., Guseva N. G., Fricke K. J., Henkel C., 2011, A&A, 533, A25
Kinman T. D., 1965, ApJ, 142, 1241
Koss M. et al., 2014, preprint (arXiv:1401:6798v1)
,Kramida A., Ralchenko Yu., Reader J. NIST ASD Team 2012, NIST Atomic Spectra Database (version 5.0), available at: http://physics.nist.gov/asd
Kunth D., Östlin G., 2000, A&AR, 10, 1
Lee H., Grebel E. K., Hodge P. W., 2003, A&A, 401, 141
Leitherer C., Heckman T. M., 1995, ApJS, 96, 9
Leitherer C. et al., 1994, ApJ, 428, 292
Macchetto F., Colina L., Golombek D., Perryman M. A. C., di Serego Alighieri S., 1990, ApJ, 356, 389
Mas-Hesse M. J., Kunth D., Tenorio-Tagle G., Leitherer C., Terlevich R. J., Terlevich E., 2003, ApJ, 598, 858
Melnick J., Tenorio-Tagle G., Terlevich R., 1999, MNRAS, 302, 677
Mollá M., García-Vargas M. L., Bressan A., 2009, MNRAS, 398, 451
Morton D., 1991, ApJS, 77, 119
Mould J. R. et al., 2000, ApJ, 529, 786
Nazé Y., Rauw G., Hutsemékers D., 2012, A&A, 538, A47
Petit V., Drissen L., Crowther P. A., 2006, AJ, 132, 1756
Pilyugin L. S., Ferrini F., Shkvarun R. V., 2003, A&A, 401, 557
Roy J.-R., Aube M., McCall M. L., Dufour R. J., 1992, ApJ, 386, 498
Sandage A., 1971, ApJ, 166, A70
Silich S., Tenorio-Tagle G., Rodríguez-González A., 2007, ApJ, 610, 226
Smith C. L., Fanelli M., Marcum P., 2007, Am. Astron. Soc. Meeting Abstr. 9, 993
Smith N., Li W., Silverman J. M., Ganeshalingam M., Filippenko A. V., 2011, MNRAS, 415, 773
Stasińska G., Cid Fernandes R., Mateus A., Sodré L., Asari N. V., 2006, MNRAS, 371, 972
Tenorio-Tagle G., Silich S. A., Kunth D., Terlevich E., Terlevich R., 1999, MNRAS, 309, 332
Tenorio-Tagle G., Wünsch R., Silich S., Palous J., 2007, ApJ, 658, 1196
Terlevich R., 1994, in Clegg R. E. S., Stevens I. R., Meikle W. P. S., eds, Proc. 34th Herstmonceux Conf., Circumstellar Media in Late Stages of Stellar Evolution. Cambridge Univ. Press, Cambridge, p. 153
Terlevich E., Díaz A. I., Terlevich R., 1990, MNRAS, 242, 271
Terlevich R., Tenorio-Tagle G., Franco J., Melnick J., 1992, MNRAS, 255, 713
Terlevich E., Díaz A. I., Terlevich R., González-Delgado R. M., Pérez E., García Vargas M. L., 1996, MNRAS, 279, 1219
The Chandra Proposers' Observatory Guide, Issue 16.0, 2013, Chandra X-ray Center, available at: http://cxc.harvard.edu/proposer/POG/
Turatto M., 2005, in Weiler K., ed., Lecture Notes in Physics, Vol. 598, Supernovae and Gamma-Ray Bursters. Springer-Verlag, Berlin, p. 21
Turatto M., 2005, in Marcaide J. M., Weiler K. W., eds, Springer Proc. Phys. Vol. 99, IAU Colloq. 192: Cosmic Explosions, On the 10th Anniversary of SN1993J. Springer-Verlag, Berlin, p. 151
Tutukov A. V., 1978, A&A, 70, 57
Vernet J. et al., 2011, A&A, 536, A105

This paper has been typeset from a TEX/LATEX file prepared by the author.